Tutor/s

Dr. Javier Fernández
Departament de Química de Materials i Química Física

Grau de Química

Treball Final de Grau

Reduction and characterization of the band gap of TiO_2 nanoparticles

Reducció i caracterització de la banda prohibida de nanopartícules de TiO_2

Albert de Pablo i Quesada

Juny 2021

UNIVERSITAT DE BARCELONA

B:KC Barcelona Knowledge Campus
Campus d'Excel·lència Internacional

When it is obvious that the goals cannot be reached,
do not adjust the goals, adjust the action steps.

Confucius

En primer lloc, vull agrair a la Noemí Gavieiro per haver-me ajudat des del primer moment fins al darrer en el desenvolupament del treball. Per descomptat també agrair al Javier, a la Raisha, i a l'Alda per haver-me donat un cop de mà sempre que ho he necessitat. Així també al departament de Ciència de Materials i Química Física de la UB, al CPT i al CCiTUB per haver-me proporcionat totes les instal·lacions, materials, reactius i equips necessaris per dur a terme tots els experiments i caracteritzacions.

També agrair a la meva família per haver-me donat suport durant tot aquest temps, a la Maria per estar al meu costat durant el darrer any i a tots els meus amics per haver contribuït a ser la persona que sóc avui en dia.

REPORT

CONTENTS

1. SUMMARY

The increase of pollution in both air and water due to anthropogenic causes, especially in large cities, is a tendency that should be reverted. Many of these pollutants can be degraded through the absorption of solar energy by a photocatalyst. Titanium dioxide (TiO_2) is a semiconductor that can act as a photocatalyst when absorbing light from the UV region of the spectrum (100-400 nm), which only represents 4-6% of sunlight. To make the most of the sun's energy, and to be able to apply this process efficiently on a large scale, black TiO_2, which can absorb practically the entire range of the solar spectrum, has been synthesized. In this work, TiO_2 nanoparticles are synthesized by sol-gel method and different treatments are applied to obtain black TiO_2. Finally, the products obtained are characterized by FESEM, Raman spectroscopy, XRD and Photoluminescence Spectroscopy, and compared to commercially available TiO_2 nanoparticles. Moreover, the degradation of an organic molecule in presence of an aqueous suspension of TiO_2 inside a solar simulator is studied to test out the photocatalytic efficiency of the products.

Keywords: Nanoparticles, photocatalysis, black TiO_2.

2. RESUM

L'augment de la contaminació tant de l'aire com de l'aigua per causes antropogèniques, sobretot a les grans ciutats, és una tendència que s'ha de revertir. Bona part dels contaminants poden ser degradats mitjançant l'absorció d'energia solar per part d'un fotocatalitzador. El diòxid de titani (TiO_2) és un semiconductor que pot actuar com a fotocatalitzador quan absorbeix llum de l'espectre UV (100-400 nm), el qual representa un 4-6% de la llum solar. Per tal d'aprofitar el màxim possible l'energia del sol i poder aplicar aquest procés a gran escala de manera eficient s'ha sintetitzat el TiO_2 negre, el qual és capaç d'absorbir pràcticament tot l'espectre solar. En aquest treball es sintetitzen nanopartícules de TiO_2 i s'apliquen diferents tractaments per tal d'obtenir el TiO_2 negre. Posteriorment es caracteritzen els productes obtinguts pel FESEM, espectroscòpia Raman, difracció de raigs X i per espectroscòpia de fotoluminescència i es comparen amb el TiO_2 comercial. A més a més, s'estudia la degradació d'una molècula orgànica en presència d'una suspensió aquosa de TiO_2 dins d'un simulador solar, per tal de posar a prova l'eficiència fotocatalítica dels productes.

Paraules clau: Nanopartícules, fotocatàlisi, TiO_2 negre.

3. INTRODUCTION

The scientific community is facing a big challenge since air and water pollution have not stopped rising in the last years due to the massive growth of industry. Studies are being carried out in order to minimize the impact of pollutants to the world and therefore slow down climate change [1].

An efficient and green way to solve this problem is by using nanoparticles (NPs) acting as photocatalysts, which can oxidize most of the pollutants present in the air and even destroy bacteria and fungus just by using sunlight. Titanium dioxide (TiO_2) NPs have been the focus of research studies, but the main issue is that they are only active as photocatalysts when absorbing light from the UV spectrum (100-400 nm), which only represents 4-6% of the sunlight [2]. The introduction of surface disorders in TiO_2 can make its light absorption properties increase to the point that even Near Infrared (NIR) region of solar spectrum is useful (780-2500 nm) [2]. These changes and enhanced properties are usually related to a change in the colour of TiO_2, being the black the most studied [3].

3.1 NANOPARTICLES

Nanoparticles are commonly described as particles with a diameter between 1 to 100 nm, or that have at least one dimension in the nanometre scale, as the prefix “nano” denotes a factor of 10^{-9}, meters in this case.

Nanomaterials (NMs), which are materials containing NPs, can be organized into 4 categories depending on their chemical composition: carbon-based, organic-based, composite-based and inorganic-based, being the latter the one concerned as it includes TiO_2. NMs can also be classified basing on their dimensions and their origin: natural or synthetic [4].

What makes this area of research attractive is the fact that properties of NMs are different from the equivalent chemical compound in a micro or macro scale. When the size of a particle is reduced, the surface/volume increases and the contribution of surface atoms becomes crucial, therefore the object shows new chemical, optical, electric and magnetic properties [5]. Thus, the

interest for the study of nanoparticles and nanomaterials (NMs) has increased in the last decades developing what is called nanoscience and nanotechnology.

Nevertheless, Egyptians and Mesopotamians started using NPs for obtaining a glittering effect in ceramic vessels back in the 13th and 14th century BC. Many other civilizations have used NPs through ages for different purposes such as cosmetics, hair dyes or decoration. Although the most famous example is the *Licurgus Cup* made by Romans in the 4th century AD which resembles different colours whether it is illuminated from the inside or from the outside [5].

3.2 PHOTOCATALYSIS

The term photocatalysis is composed by 2 words: photo and catalysis, therefore it is a process in which a substrate absorbs light and changes the rate of a chemical reaction. These substrates are known as photocatalysts and almost all of them are semiconductors, such as TiO_2, due to their electronic structure [6].

Photocatalysis can be categorized into 2 different types depending on the physical state of reactants: Homogenous, when the semiconductor and reactant are in the same phase, and heterogenous when they are in different phases [6].

It consists of 3 main steps: light absorption, electron hole separation and surface reaction [2]. In order for it to work, the energy of the irradiating light must be the same or higher than the energy of the band gap of the substrate so the electrons from the Valence Band (VB) can absorb photons ($h\nu$) and excite to the Conduction Band (CB) (equation 1). The band gap is precisely the energy between the VB and the CB [6]. When this process occurs, positive holes (h^+) are created in the VB, and photogenerated electrons (e^-) in the CB, which can take part in oxidation and reduction reactions respectively (figure 1). While the holes can react with H_2O to form hydroxyl radicals (*OH), electrons can react with O_2 to yield superoxide radicals (O_2^-*) (equations 2 and 3 respectively). These free radicals are responsible for the degradation of pollutants via a redox reaction (equations 4 and 5) [2].

$$Photocatalyst + h\nu \rightarrow h_{VB}^+ + e_{CB} \quad (1)$$

$$H_2O + h_{VB}^+ \rightarrow {}^*OH\ (hydroxyl\ radical) + H^+ \quad (2)$$

$$O_2 + e_{CB}^- \rightarrow O_2^-{}^*\ (superoxide\ radical) \quad (3)$$

$$^*OH + pollutant \rightarrow Intermediates \rightarrow H_2O + CO_2 \quad (4)$$

$$O_2^{-*} + pollutant \rightarrow Intermediates \rightarrow H_2O + CO_2 \quad (5)$$

*Reactions: 1) Formation of holes (h^+) and electrons (e^-), 2) Formation of the hydroxyl radical (*OH), 3) Formation of the superoxide Radical (O_2^{-*}), 4 and 5) Degradation of pollutants by radicals.*

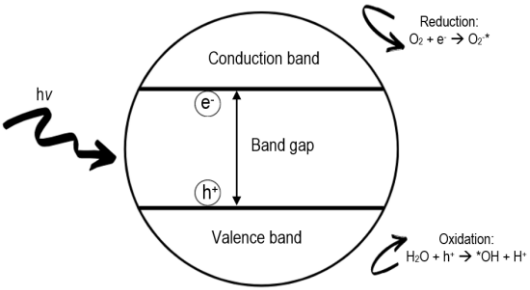

Figure 1: Photocatalytic process in semiconductors.

Photocatalysts are mainly semiconductors due to their electronic structure, which has a filled VB and an empty CB that allow the electrons to excite from the first to the second [7]. Moreover, various investigations have stablished that semiconductors in form of NPs are more effective as photocatalysts than in form of bulk powder [1].

3.3 TITANIUM DIOXIDE (TiO_2)

Titanium dioxide (TiO_2), Titanium (IV) oxide or Titania belongs to the family of transition metal oxides. TiO_2 is a very interesting compound from a scientific and technological point of view since it is chemically stable and harmless. It is also inexpensive, as Titanium is the 9th most abundant element on earth [8]. Moreover, its interesting properties are useful in a wide range of fields, including photocatalysis.

3.3.1. Structures

TiO_2 can be found in nature in 3 different crystalline structures: brookite (orthorhombic), rutile and anatase (tetragonal) [1]. Among them, rutile and anatase are the most studied ones since brookite is rare and difficult to synthesize [9]. Rutile and anatase contain 6 and 12 atoms per cell, respectively. In both structures, each Ti atom is coordinated to 6 O atoms, and each O atom is coordinated to 3 Ti atoms at the same time [10]. The basic unit-cells of the three structures are shown in figure 2.

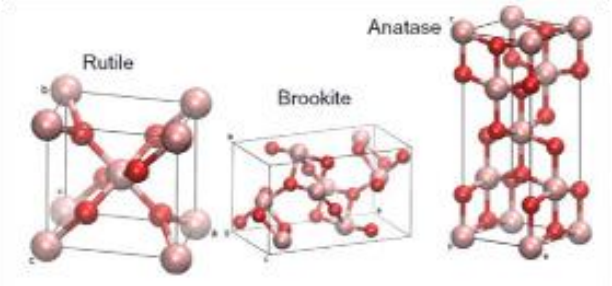

Figure 2: crystalline structures of TiO_2 rutile, brookite and anatase, respectively.

Even though the band gap of anatase (3,2 eV) is higher than the rutile band gap (3,0 eV), the photocatalytic performance of anatase is considered superior [11]. This is attributed to a higher electron mobility, low dielectric constant and lower density [1]. However, it is known that a phase mixture of the two different polymorphs has a synergetic effect and increases the photocatalytic activity of TiO_2 [12]. All the crystal parameters and properties of each polymorph are summed up in table 1 [10,13].

	Rutile	**Anatase**	**Brookite**
Crystal structure	Tetragonal	Tetragonal	Orthorhombic
Lattice constants (Å)	a = b = 4,5936 c = 2,9587	a = b = 3,784 c= 9,515	a = 9,1854 b = 5,447 c = 5,154
Molecule/cell	2	4	8
Volume/molecule (Å)	31,2160	34,061	32,172
Density (g/cm^3)	4,13	3,79	3,99
Dielectric Constant (ε)	114	31	---
Band gap (eV)	3,0	3,2	3-3,6

Table 1: Crystal parameters and properties of rutile, anatase and brookite polymorphs.

3.3.2. Synthethic methods

There are different ways of synthesizing nano-TiO_2 depending on the final properties required. Focusing on obtaining TiO_2 for photocatalytic applications, the most used methods are hydrothermal, sonochemical and sol-gel synthesis [14].

Hydrothermal synthesis is used for obtaining small particles and it is usually conducted in autoclave under controlled atmospheric conditions. It consists of dissolving a metallic precursor in a liquid and heating above its boiling point so it reaches to saturated vapor pressure [14].

Sonochemical synthesis has been used for synthesizing nanostructured materials including colloids, alloys, oxides, carbides and transition metals with a high surface area [14]. It is based on sonochemistry, which consists of irradiation of high intensity ultrasounds producing acoustic cavitation. These conditions produce unique hot spots that can achieve temperatures above 5000K and pressures of 1000atm with a very high cooling rate, forcing the reaction to occur [15].

The sol-gel method is based on the hydrolysis and polymerization of a precursor, in this case a metal alkoxide (titanium isopropoxide or titanium butoxide) in an organic solution. This precursor is hydrolyzed under ambient conditions forming a colloidal suspension named sol, in which the particles are dispersed [16]. The loss of solvent connects these particles and completes the polymerization reaction transforming the sol into a gel. This gel is heated until all the organic compounds are evaporated leaving the desired metal oxide [16]. This process is schematized in scheme 1, where we can see the mechanism of the polymerization reaction of titanium isopropoxide [17].

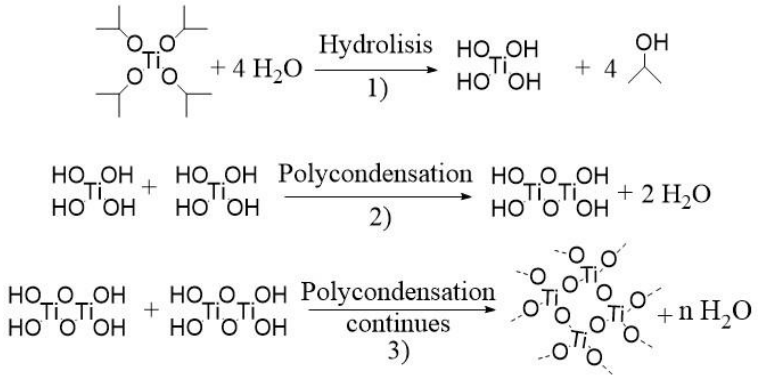

Scheme 1: Representation of titanium isopropoxide polymerization reaction made with ChemDraw: 1) Hydrolysis, 2) Polycondensation and 3) End of polycondensation and formation of the gel.

This method is very important for the fabrication of functional materials such as photocatalysts, and also for nanotechnology, since nanospheres and nanofibers can be formed during this process [16].

3.3.3. Applications

TiO_2 has been used historically as a white pigment in paints, plastic and paper among others, as it has no absorption in the visible region of the spectra [8]. However, nowadays the variety of its applications range from common products such as sunscreens to more complex devices to be used even as a biomaterial due to its biocompatibility [18]. Nevertheless, since it is considered the most promising material for harvesting light, it has been investigated for different purposes such as photodegradation [19,20], dye sensitized solar cells [21,22], self-cleaning surfaces [23,24], solar water splitting [25–27], organic reactions [28], photocatalytic sensors [29,30] etc. We will focus on its photocatalytic applications for self-cleaning surfaces.

3.3.3.1. TiO_2 as a photocatalyst

Back in 1972, Honda and Fujishima reported that a photoanode of TiO_2 has the capability to split water into H_2 and O_2 under UV light radiation by a photocatalytic reaction as in equations 7 and 8 [31].

$$2H^+ + 2e_{CB}^- \rightarrow H_2 \quad (7)$$

$$2H_2O + 4h_{VB}^+ \rightarrow O_2 + 4H^+ \quad (8)$$

Equations: 7) Oxidation of H+ to form H_2 by photogenerated electrons (e-), 8) Reduction of water to form O_2 by photogenerated holes (h+).

Since then, photocatalysis has attracted a lot of interest and TiO_2 has become the most investigated and promising photocatalyst. However, there are some issues yet to be solved, as its wide band gap (3,0-3,2 eV) limits its ability to harvest sunlight [32]. Moreover, the positive holes (h^+) and the photogenerated electrons (e^-) (which together form an exciton) can rapidly recombine due to surface and bulk defects, releasing energy in the form of heat or photons as shown in equation 9, and therefore decreasing the photocatalytic activity [33].

$$h_{VB}^+ + e_{CB}^- \rightarrow \text{energy (heat)} \quad (9)$$

Equation 9: Recombination of holes (h^+) and photogenerated electrons (e^-).

These limitations encouraged the scientific community to enhance the photocatalytic efficiency of TiO_2 by employing different methodologies. Metal and non-metal doping have been considered. Nevertheless, while metal doping generated secondary impurities, non-metal doping was unable to absorb light from IR region (780nm-1mm), which covers a 52% of the solar spectrum [34].

3.3.4. TiO_2 colours

Since TiO_2 has been the focus of many experiments, different colours have been reported although pristine TiO_2 is white. Yellow [35,36], red [37], blue [38,39] grey [40], brown [41] and black TiO_2 [2,33,42–47] have been synthesized, being the later the one most likely to be used for photocatalytic purposes, since its band gap is much narrower [2]. The change in colours is related to defects on its crystalline structure such as formation of Ti-H bonds, surface OH groups, oxygen vacancies and Ti^{3+} species [2]. Thus, terms such as "Hydrogenated TiO_2", "Reduced TiO_2" and "TiO_{2-x}" have also been employed for non-black samples with enhanced photocatalytic activity [2].

3.3.4.1 Black TiO_2

The term "black TiO_2" was first used by Chen et al. in 2011, when white TiO_2 was hydrogenated in a 20.0 bar H_2 atmosphere at 200ºC for 5 days yielding a black product [47]. This discovery revolutionized the research for photocatalysts as black TiO_2 possesses a narrower band gap (1,5 eV) and can absorb the entire range of solar spectra without the addition of any dopant [14,34]. These enhanced photocatalytic properties are mainly attributed to oxygen vacancies and the formation of Ti^{3+} species, which create non-paired electrons that can excite to the CB. However, some studies report that an excess of these defects can make the photocatalytic activity decrease as they may act as recombination centres [48].

3.3.5. Synthesis routes of black TiO_2

In order to find the most suitable, green and economic synthesis for industrializing black TiO_2 nanomaterials, different strategies have been employed. The most studied route is hydrogenation, which is based on introducing defects on TiO_2 structure by heating at elevated temperatures under a reducing atmosphere consisting of H_2 [49], H_2/Ar [50], H_2/N_2 [51], or Ar [52]. Other studied methods include electrochemical reduction [53], chemical oxidation/reduction [45,54], plasma assisted process [55], laser ablation [46], ionothermal treatment [56], ultrasonication [42], etc. All

these synthesis routes are summed up in figure 3 and are based on the reduction of TiO_2, as shown in equation 10, where red represents the reductant:

$$TiO_2 + Red \rightarrow TiO_{2-x} + RedOx \quad (10)$$

Equation 10: TiO_2 generic reduction reaction.

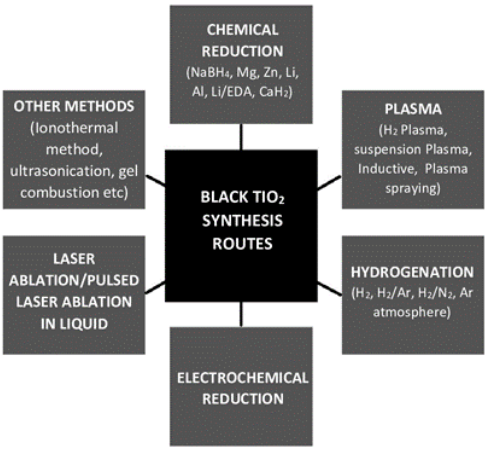

Figure 3: Synthesis routes of black TiO_2.

3.3.5.1 $NaBH_4$ reduction

Sodium borohydride ($NaBH_4$) is a typical reducing agent, widely used in organic chemistry. In what concerns to TiO_2 reduction, $NaBH_4$ has the capability to reduce Ti^{4+} to Ti^{3+} as in equations 11 and 12, producing in situ H_2 at room temperature, which then can convert white TiO_2 into black [45].

$$NaBH_4 + 8OH^- \rightarrow NaBO_2 + 8e^- + 6H_2O \quad (11)$$

$$Ti^{4+} + e^- \rightarrow Ti^{3+} \quad (12)$$

$$BH_4^- + 2H_2O \rightarrow BO_2^- + 4H_2 \quad (13)$$

Equations: 11) $NaBH_4$ oxidation, 12) Ti^{4+} reduction and 13) Formation of boron oxide species (BO_2^-).

During this process, boron oxide species are produced due to their insolubility in organic solvents, but they can be washed out by HCl solution which removes surface impurities, increasing the visible light absorption of TiO_2 [45,57].

4. OBJECTIVES

The main objective of this project is to synthesize TiO_2 NPs with a narrower band gap so they can be used for photocatalytic applications. To accomplish it, the following steps are followed:

- Synthesis of TiO_2 nanoparticles by sol-gel method.
- Stabilization of the crystalline structure.
- Obtention of reduced TiO_2 by heat and chemical treatments.
- Characterization of the obtained products.
- Process improvement.

5. EXPERIMENTAL SECTION

5.1. MATERIALS

The chemicals used in these experiments were 2-propanol or isopropanol (≥99,5%, Sigma-Aldrich), ethanol absolute (Codex Panreac), Titanium (IV) isopropoxide (97%, Aldrich), nitric acid pure (69%, Labkem), sodium hydroxide solution (0,5mol/L, Scharlau), sodium borohydride (99%, Sigma-Aldrich), titanium oxide anatase powder and rutile titanium oxide powder off-white (Sulzer), Titanium dioxide Degussa P25 (Evonyk), sulfamethoxazole (Sigma Aldrich).

5.2. SYNTHESIS OF TiO_2 NANOPARTICLES

The sol-gel method is the one employed for synthesizing TiO_2 nanoparticles. Titanium (IV) isopropoxide (TTIP) is used as the alkoxide precursor, and the organic solvent varies from ethanol to isopropanol. In both cases, two solutions are prepared: Solution A is composed of 50 ml of TTIP and 50ml of the organic solvent, and solution B is formed by 100 ml of the same organic solvent (1:3 relation between precursor and solvent) and 1 ml of HNO_3 which acts as an acid catalyst. Solution A is added dropwise to solution B and the resulting mixture is stirred for approximately 2 hours at room temperature. Later it is transferred into a beaker to stimulate evaporation and it is heated at 100 ºC until the solvent is evaporated leaving a powder, which then is placed in a heater to eliminate any remaining humidity. This process can be seen in figure 4.

$$Ti(iPrO_4) + H_2O \xrightarrow{1} Ti(OH)_4 \xrightarrow{2} TiO_2 \cdot 2H_2O \xrightarrow[\Delta]{3} TiO_2$$

Figure 4: Sol-gel synthesis steps and reactions: 1) Hydrolyzation, 2) Polymerization and 3) Drying.

After obtaining the dried powder, two heat treatments are carried out by heating it at 500 ºC for 4h in different ovens. The first treatment is done under an oxidant atmosphere (normal air) to stabilize the crystalline structure. The second one is conducted under a reductant atmosphere consisting of N_2 to induce oxygen vacancies to minimize the band gap (figure 5).

Figure 5: TiO_2 synthesized by sol-gel method after heat treatment under oxidant atmosphere (left) and after treatment under reductant atmosphere (right).

Different amounts of the chemical reductant ($NaBH_4$) have also been added to the solution to reduce titania and avoid the second heat treatment [57]. Washing with a 1 M HCl solution and neutralizing by dialysis for one week which assists the formation of the gel (figure 6) have also

been carried out afterwards. By dialysis, not only the formation of gel is induced, but also the remaining ions are washed out.

Figure 6: Dialysis tubing after neutralizing for 1 day (left) and for 1 hour (right).

Other variations such as the addition of 20 ml of 1 M NaOH solution or 20 ml of deionized water have been tried to form a precipitate that assists the formation of the gel by a polymerization reaction.

5.2.1. Reduction of rutile and anatase powders

Aside from the sol-gel synthesis and its variants, chemical reduction of commercially available TiO_2 powders with $NaBH_4$ under a reductant atmosphere has also been carried out. To do so, 3 g of TiO_2 (anatase and rutile separately) were mixed thoroughly in a mortar with 0,3 g of $NaBH_4$ and then placed in an oven at 500 ºC for 4h under a reductant atmosphere (N_2) [48].

Figure 7: TiO_2 rutile (above) and anatase (below) mixed with $NaBH_4$ before (left) and after (right) the heat treatment under a reductant atmosphere.

5.3. PHOTOCATALYTIC DEGRADATION OF SULFAMETHOXAZOLE BY TiO_2

To test out the photocatalytic efficiency of TiO_2, the photodegradation of sulfamethoxazole (SMX) in aqueous suspension of TiO_2 was studied. The experimental set-up consisted of a 600 ml pyrex beaker used as a reactor containing 500 ml of a SMX solution of 3 mg/L with constant magnetic stirring (figure 8). The beaker was placed inside a solar simulation chamber (Xenoterm-1500RF, CCI), which uses a Xenon lamp (1,5 kW) as a source of radiation with a spectrum very close to the solar in the UV range. An initial sample was taken before the addition of 0,125 g of TiO_2 anatase powders to the solution and another after stirring for 20 minutes. Afterwards, the lamp was turned on for 3 hours, taking samples every 15 minutes during the 1st hour, every 30 minutes during the 2nd hour, and 1 after 3 hours. This experiment was carried out with commercially available TiO_2 anatase powders before and after the heat treatment with $NaBH_4$ under a reductant atmosphere, and with Degussa P25 TiO_2 which contains 80% of anatase and 20% of rutile.

Figure 8: Experimental set-up of the photodegradation of sulfamethoxazole in aqueous suspension of TiO_2 inside a Solar Simulator.

5.4. CHARACTERIZATION

Scanning Electron Microscope (JEOL JSM-5310 SEM) equipment was employed to determine the morphology and surface composition of the particles. It was used with a potential of 20KV, working with secondary electron images and an X-ray detector (EDS) for composition determination, which in this case is useful to find out if there is contamination in our samples.

Field Emission Electron Microscope (FESEM JEDL J-7100) was also used to provide images with higher resolution.

The phase composition and crystallinity of the particles were determined by Raman spectroscopy (HORIBA JOBIN YVOS Lab RAM HR). The spectrum was recorded using a green laser of a wavelength of 523 nm, with a 10% power. An objective of 50 was used to focus the laser beam on the sample surface for an exposure time of 10 seconds each time. The detector used was a NIR enhanced Deep Depletion CCD array, which was Peltier cooled to -65 ºC.

To determine the crystallographic structure of TiO_2, X-Ray Diffraction (XRD) analysis was performed. The samples were loaded in standard cylindrical sample holders of 16 mm of diameter and 2,5 mm of height with a constant spin of 2 revolutions per second. The measurements were carried out in a PANalytical X'Pert PRO MPD alpha1 powder diffractometer in Bragg-Brentano $\theta/2\theta$ geometry of 240 mm of radius. It operated in reflection mode with Cu-$k_{\alpha 1}$ radiation with a work power of 45 kV, 40 mA. Diffracted beam monochromator used a step scan mode with a step size of 0,026º and 300 seconds of measuring time.

In order to characterize the band gap of TiO_2 nanoparticles, photoluminescence spectroscopy was carried out. The samples were placed in an Eppendorf tube and were irradiated with an IK series He/Cd laser at 325 nm. The spectrum was recorded over the range of 350-650 nm. However, some issues were found as irradiating at higher wavelengths degraded the tube.

The concentration of SMX solutions were measured by using Infinity 1260 HPLC apparatus, provided by Agilent Technologies. A Mediterranean Sea column was employed (250 mm x 4,6 mm and 5 µm particle size) supplied by Teknokroma. The mobile phases consisted of volumetric mixtures containing 50% of acetonitrile and 50% of pure water adjusted at pH 3 with orthophosphoric acid. The flux used was 1,1 ml min^{-1} and the UV detector was set at 270 nm. The injection volume was 50 µL and the temperature was set to 30 ºC.

6. CHEMICAL CHARACTERIZATION

The morphology of TiO_2 NPs synthesized by sol-gel has been compared before and after the two heat treatments (figure 9). Before any heat treatment (figure 9.A), NPs cannot be distinguished as the phase has not been stabilized yet. After the heat treatment under oxidant atmosphere, agglomerated NPs can be observed (figure 9.B) and finally after all the heat treatments, there are spheric and distinguishable NPs (figure 9C). These experimental results are compared to commercially available anatase before and after the heat treatment with $NaBH_4$ (figure 9.D and 9.E respectively). In this case, heat treatment under an oxidant atmosphere is not required since the phase is already stabilized.

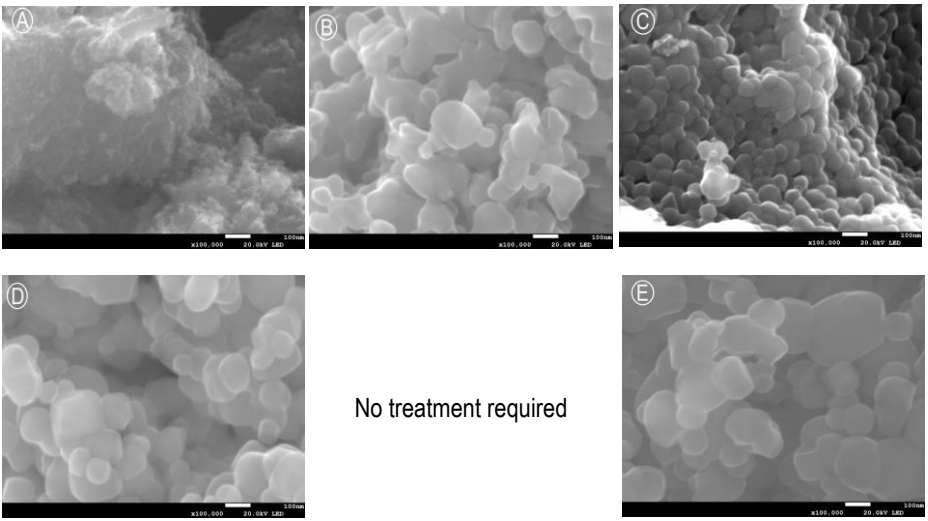

Figure 9: FESEM pictures of TiO_2 synthesized by sol-gel method with isopropanol, pH change (NaOH) and dialysis neutralization: A) Before any heat treatment, B) after 4 hours at 500 ºC under an oxidant atmosphere, C) after 4 hours at 500 ºC under N_2 atmosphere. Below there are pictures of commercially available anatase: D) Without any treatment. E) After heat treatment with $NaBH_4$ under N_2 atmosphere.

As we can observe in figure 10.A, the size of the TiO_2 NPs synthesized by sol-gel ranges from 30 to 80 nm. On the other hand (figure 10.B), the average size of commercially available anatase NPs is over 100 nm. Therefore, the sol-gel method not only produces NPs, but also these NPs are smaller than the commercially available.

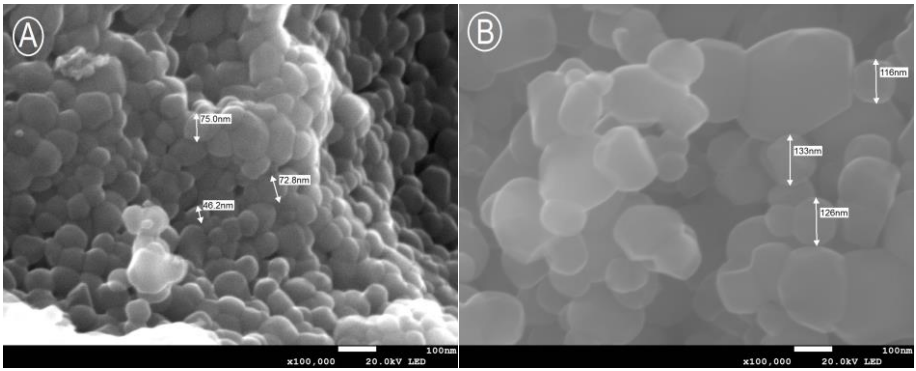

Figure 10: Size of the TiO_2 nanoparticles: A) Synthesized by sol-gel method and B) Commercially available anatase.

An EDS was also done to confirm that the sample is TiO_2 and discard the presence of any impurities (figure 11). This spectrum is representative of all the samples except to those reduced with $NaBH_4$, which had remaining Na^+ contamination. Thus, washing with HCl 1 M and with deionized water was necessary to eliminate these ions.

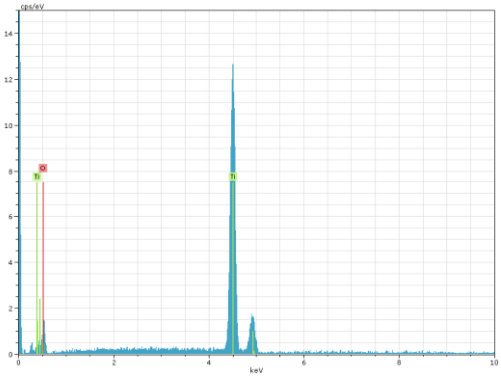

Figure 11: EDS spectrum of synthesized TiO_2.

In figure 12, the morphology of the NPs synthesized by the different methods are compared after all heat treatments. The main difference between the use of ethanol or isopropanol as the organic solvents is the particle shape. As we can see in figure 12.A, and 12.B and 12.C, the particles are not as spherical as those obtained using isopropanol (figure 12.D, 12.E, and 12.F). Thus, by using isopropanol as organic solvent, the size and the shape of NPs is controlled. Nevertheless, NPs were obtained with both solvents. Although addition of $NaBH_4$ to the solution (figure 12.C) did not reduce titania, agglomerated NPs were still formed. The boron oxide species generated may have acted as a nucleus for the NPs to grow [58].

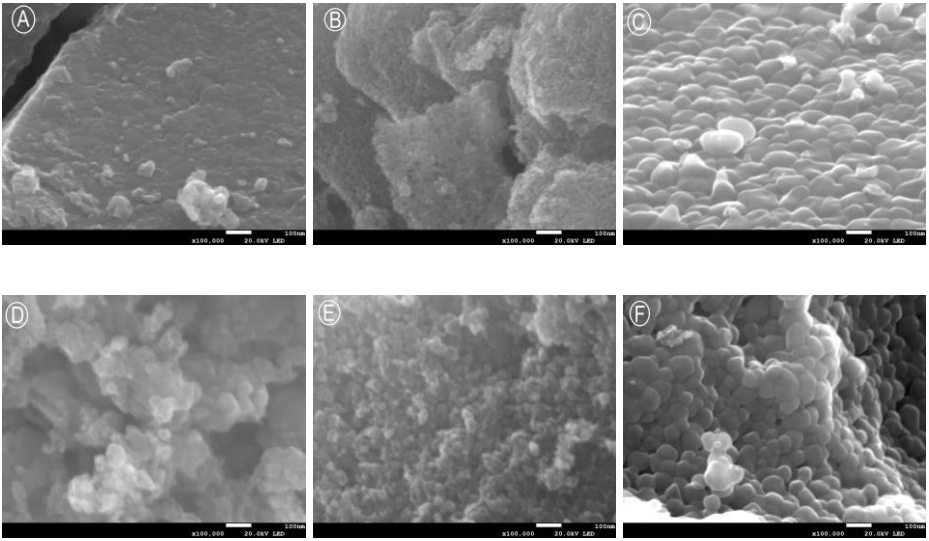

Figure 12: FESEM pictures of TiO_2 NPs synthesized by sol-gel after all the heat treatments: A) EtOH as organic solvent and pH change with H_2O, B) EtOH and pH change with NaOH, C) EtOH and addition of $NaBH_4$ D) Isopropanol E) Isopropanol and pH modification with H_2O and F) Isopropanol, pH modification with NaOH and dialysis neutralization.

7. STRUCTURAL DETERMINATION

Raman spectrum (figure 13) reveals structural information of commercially available anatase and rutile. Four Raman active modes for anatase TiO_2 polymorph with symmetries E_g, B_{1g}, A_{1g} and E_g are observed at 140, 395, 513 and 637 cm^{-1} respectively. On the other hand, there are three Raman active modes in the rutile phase with symmetries B_{1g}, E_g and A_{1g}, which are observed at 140, 448 and 607 cm^{-1} respectively. Moreover, there is an additional broad characteristic peak at 236 cm^{-1} which does not correspond to a vibrational frequency. It arouses from the multiple phonons scattering processes in rutile polymorph [59]. Therefore, we can confirm that the commercially available phases are indeed anatase and rutile TiO_2 [60].

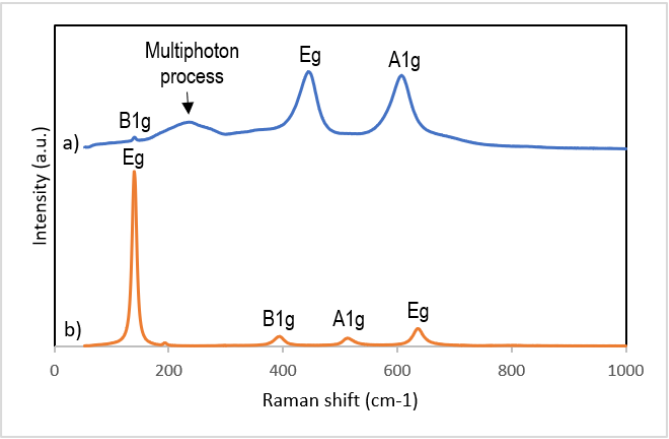

Figure 13: Raman spectrum of commercially available a) rutile (blue) and b) anatase (orange).

The crystalline structure obtained after heating TiO_2 at 500 ºC for 4 hours under atmospheric pressure is anatase [61]. This phenomenon is confirmed experimentally as we can see in the Raman spectra of TiO_2 synthesized by sol-gel method (figure 14). Before any heat treatment, there is a linear Raman shift without any intensity, which means that the phase has not been stabilized yet. However, after the oxidant heat treatment there are four peaks observed at 147,

396, 515 and 639 cm^{-1} corresponding to those of anatase. After heating under a reductant atmosphere, there are the same four peaks, confirming the presence of anatase. However, the lower intensity may mean that oxygen vacancies were induced causing crystal domain size and non-stochiometric defects [44].

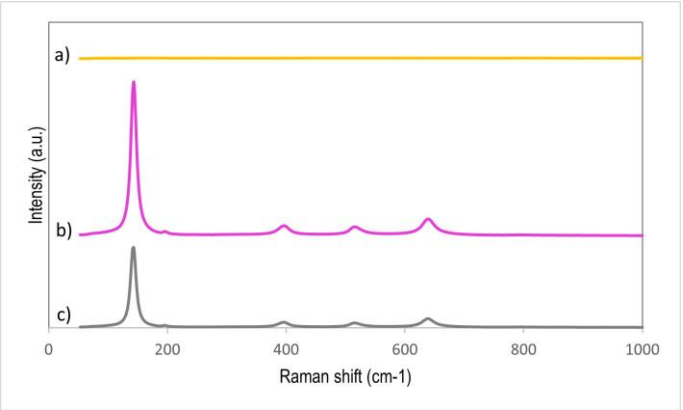

Figure 14: Raman spectrum of TiO_2 synthesized by sol-gel: a) Before any heat treatment (yellow), b) After 4 hours at 500 ºC under an oxidant atmosphere (pink), c) After 4 hours at 500 ºC under a reductant atmosphere (grey).

XRD patterns of commercially available rutile TiO_2 before and after the heat treatment are shown in figure 15. Both samples exhibit strong diffraction peaks at 27º, 26º and 55º corresponding to (110), (001) and (211) crystallographic planes, indicating that there is TiO_2 in the rutile phase [62]. These peaks were compared to the standard spectra of rutile (21-1276 JCPDS) with MAUD program. A Rietveld refinement was done to determine the structural parameters more precisely. However, after the heat treatment, two additional peaks appear that could not be identified.

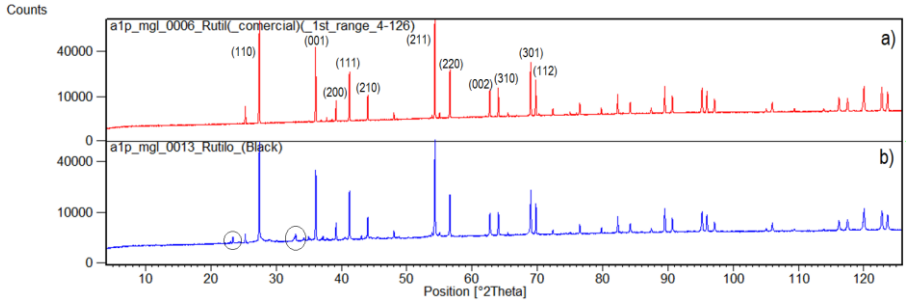

Figure 15: XRD spectra obtained with X'Pert of a) Rutile (red) and b) Rutile after the heat treatment with $NaBH_4$ under a reductant atmosphere (blue).

TiO_2 synthesized by sol-gel was also characterized by XRD and compared to that of pure anatase (figure 16). Before the heat treatment any peak can be identified due to the absence of a crystalline structure. After the heat treatment under an oxidant atmosphere, strong diffraction peaks are observed at 25º and 48º, indicating the presence of anatase phase [62], and thus confirming the results obtained by Raman spectroscopy. Pure anatase exhibits the same peaks which are in good agreement to its standard spectra (21-1272 JCPDS). However synthesized TiO_2 shows wider peaks, which means that its crystallinity is lower compared to pure anatase. These spectra have not been compared to anatase after the heat treatment with $NaBH_4$ because the results have not arrived yet.

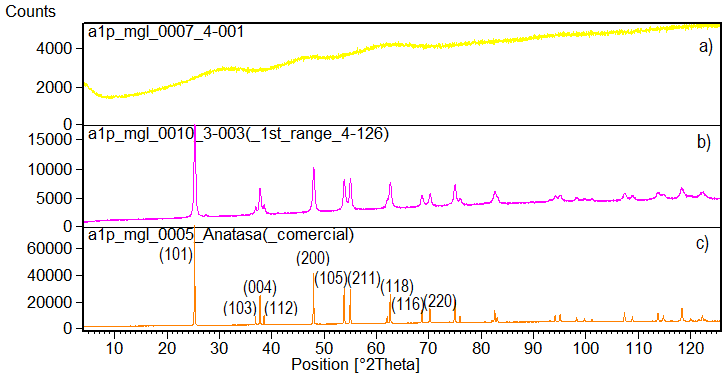

Figure 16: XRD spectra of TiO_2: a) Synthesized by sol-gel method without any further treatment (yellow), b) Synthesized by sol-gel after heat treatment under an oxidant atmosphere (pink) and c) Commercially available anatase (orange).

8. BAND GAP AND PHOTOCATALYSIS

In photoluminescence (PL) spectroscopy, the electrons from the VB are excited to the CB by the laser (hν) generating h^+ and e^- (excitons). The energy liberated after their recombination is captured by the detector as a wavelength. By using the formula in equation 14, the energy of the photons emitted can be calculated, which corresponds to the energy of the band gap, usually expressed in eV.

$$E = \hbar \cdot \frac{c}{\lambda} \quad (14)$$

Equation 14: Energy of the photons emitted after the recombination of h^+ and e^-, where $\hbar$ is Planck constant ($4{,}13 \times 10^{-15}$ eV), c is the speed of light ($2{,}99 \times 10^{8}$ m s^{-1}), and λ is the wavelength captured by the detector.

Figure 17 shows the PL spectrum of TiO_2 rutile before and after the heat treatment with $NaBH_4$. The peaks with higher intensity correspond to the energy of the band gap. Rutile without any further treatment shows a peak at λ=413 nm, which corresponds to the band gap of TiO_2 rutile (3,0 Ev). On the other hand, after the heat treatment with $NaBH_4$, a peak is observed at higher wavelengths, corresponding to a band gap of 2,5 eV, indicating that the structure has been reduced. This reduction in the band gap may be caused by the incorporation of nitrogen into the TiO_2 lattice, forming a new mid gap energy state (N 2p) which eventually decreases the band gap and shifts the optical absorption to the visible light region [63]. This would mean that TiO_2 was doped with nitrogen rather than being reduced by $NaBH_4$.

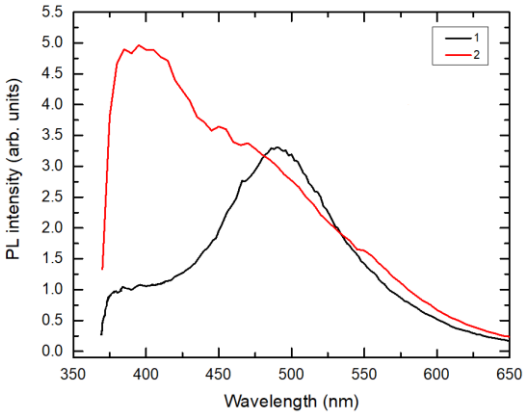

Figure 17: PL spectrum made with Origin program of 1) Pure rutile and 2) Rutile after the heat treatment under reductant atmosphere with $NaBH_4$.

Organic molecules such as SMX can be degraded by heterogeneous photocatalysis [64]. SMX is a common antibiotic, frequently found in the aquatic environment as a micropollutant [65]. In this experiment it is used as a model organic compound to study its photodegradation.

As shown in figure 18, concentration of SMX remains constant before turning on the light of the solar simulator, which means that it is stable in dark conditions. After turning on the light, the concentration of SMX decreases depending on the catalyst used. In presence of TiO_2 Degussa P25, SMX is completely degraded after 2 hours (figure 18.d), which confirms that a mixture of both rutile and anatase significantly enhances the photocatalytic activity in the degradation of organic pollutants. On the other hand, pure anatase before and after the heat treatment with $NaBH_4$ degraded 90% and 80% of the SMX after 3 hours, respectively (figure 18.b and 18.c). That would mean that washing with an HCl solution to eliminate remaining boron oxide species is crucial for the catalytic performance of TiO_2. The degradation activity of TiO_2 increases up to nine times after washing the sample with an HCl solution [45]. Hopefully, results after HCl washing will be available in the oral presentation.

Photolysis process, in which the chemical substance absorbs light and degrades due to the photochemical reactions, must also be considered (figure 18.a). After 3 hours, SMX degraded 51% just by light exposure, suggesting that part of the degradation with TiO_2 as a photocatalyst was due to photolysis.

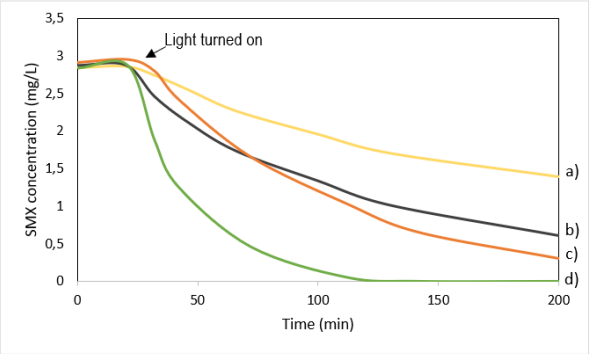

Figure 18: Degradation of SMX in aqueous suspension: a) Without any photocatalyst (yellow), b) With anatase after the heat treatment with $NaBH_4$ (black) c) Pure anatase (orange) and d) TiO_2 Degussa P25 (green).

9. CONCLUSIONS

Although the obtention of black TiO_2 NPs by chemical reduction with $NaBH_4$ in solution was not achieved, the following conclusions can be obtained:

- Suitable method for synthesizing TiO_2 NPs:
    - Sol-gel is an economic, efficient, and scalable method for the synthesis of TiO_2 NPs.
    - It has been found that the sol-gel method with addition of NaOH and dialysis neutralization generates spherical and distinguishable NPs. However, it requires long periods of time since dialysis lasts for 1 week.
    - By using isopropanol as solvent and TTIP as a precursor, the shape and the size of NPs is controlled. On the other hand, ethanol produces spiky NPs.
- Influence of heat treatments to synthesized TiO_2 NPs:
    - Heat treatment under an oxidant atmosphere is necessary to stabilize the crystalline structure of TiO_2, which is anatase after heating 4h at 500ºC.
    - By heating TiO_2 NPs at 500 ºC for 4 hours under a reductant atmosphere (N_2), grey/black TiO_2 is obtained, suggesting that vacancies are generated.
- Anatase and rutile structures
    - Rutile and anatase TiO_2 can be distinguished by XRD and Raman spectroscopy due to their different surface energies and Raman active modes.
    - A mixture of both anatase and rutile (Degussa P25) significantly enhances the photocatalytic activity of TiO_2.

- Chemical reductant ($NaBH_4$)
    - Boron oxide species in solution may act as a nucleus for NPs to grow. However reduced TiO_2 has not been generated.
    - By mixing commercially available TiO_2 rutile and $NaBH_4$ in a rate of 10:1, and heating under a reductant atmosphere of N_2 for 4 hours, the band gap is reduced to 2,5 eV due to N-doping.
    - HCl washing after $NaBH_4$ treatment to eliminate boron oxide species is crucial to enhance the photocatalytic performance of TiO_2.

10. REFERENCES AND NOTES

[1] S. M. Gupta and M. Tripathi, "A review of TiO_2 nanoparticles," *Chinese Sci. Bull.*, vol. 56(16), pp. 1639–1657, **2011**, doi: 10.1007/s11434-011-4476-1.

[2] T. S. Rajaraman, S. P. Parikh, et al., "Black TiO_2: A review of its properties and conflicting trends," *Chem. Eng. J.*, vol. 389, pp. 123918, **2020**, doi: 10.1016/j.cej.2019.123918.

[3] Y. Li, R. Fu, et al., "Preparation of core-shell nanostructured black nano-TiO_2 by sol-gel method combined with Mg reduction," *J. Mater. Res.*, vol. 33(24), pp. 4173–4181, **2018**, doi: 10.1557/jmr.2018.411.

[4] J. Jeevanandam, A. Barhoum, et al., "Review on nanoparticles and nanostructured materials: History, sources, toxicity and regulations," *Beilstein J. Nanotechnol.*, vol. 9(1), pp. 1050–1074, **2018**, doi: 10.3762/bjnano.9.98.

[5] D. Schaming and H. Remita, "Nanotechnology: from the ancient time to nowadays," *Found. Chem.*, vol. 17(3), pp. 187–205, **2015**, doi: 10.1007/s10698-015-9235-y.

[6] R. Ameta, M. S. Solanki, et al., "Photocatalysis," in *Advanced Oxidation Processes for Waste Water Treatment: Emerging Green Chemical Technology, Udaipur,* Ed. Academic Press, pp. 135-165, **2018**.

[7] D. Beydoun, R. Amal, et al., "Role of nanoparticles in photocatalysis," *J. Nanoparticle Reasearch*, vol. 1(3), pp. 439–458, **1999**, doi: 10.1023/A:1010044830871.

[8] K. Hashimoto, H. Irie, et al., "TiO_2 photocatalysis: A historical overview and future prospects," *Japanese J. Appl. Physics, Part 1 Regul. Pap. Short Notes Rev. Pap.*, vol. 44(12), pp. 8269–8285, **2005**, doi: 10.1143/JJAP.44.8269.

[9] L. Gracia and J. Andre, "Density Functional Theory Study of the Brookite Surfaces and Phase Transitions between Natural Titania Polymorphs," *J. Phys. Chem. B*, vol. 110(46), pp. 23417–23423, **2006,** doi: 10.1021/jp0643000

[10] S. Mo and W. Y. Ching, "Electronic and optical properties of three phases of titanium dioxide: Rutile, anatase and brookite," vol. 51(19), pp. 23–32, **1995.** doi: 10.1103/PhysRevB.51.13023.

[11] D. A. H. Hanaor and C. C. Sorrell, "Review of the Anatase to Rutile Phase Transformation," *J. Mater. Sci.*, vol. 46(4), pp. 855–874, **2011**, doi: 10.1007/s10853-010-5113-0.

[12] T. Luttrell, S. Halpegamage, et al., "Why is anatase a better photocatalyst TiO_2 films," *Cient. Reports*, vol. 4(1), pp. 1–8, **2014**, doi: 10.1038/srep04043.

[13] F. Mastropietro, F. Scarpelli, et al., "Mesoporous TiO_2 Thin Films: State of the Art," in *Titanium Dioxide: Material for a Sustainable Environment*, University of Calabria, Ed. Intech Open, pp. 57–80, **2018.**

[14] M. T. Noman, M. A. Ashraf, et al., "Synthesis and applications of nano-TiO_2 : a review," *Environ. Sci. Pollut. Res.*, vol. 26(4), pp. 3262–3291, **2019**, doi: 10.1007/s11356-018-3884-z.

[15] X. Hangxun, B. W. Zeiger, et al., "Sonochemical synthesis of nanomaterials," *Chem. Soc. Rev.*, vol. 42(7), pp. 2555–2567, **2013**, doi: 10.1039/c2cs35282f.

[16] S. Shigeyuki, "Sol-Gel Process and Applications," in *Handbook of Advanced Ceramics: Materials, Applications, Processing, and Properties: Second Edition*, Tokyo, Ed. Academic Press, pp. 883–910, **2013**.

[17] P. Khodaparast and Z. Ounaies, "Influence of dispersion states on the performance of polymer-based nanocomposites," *Smart Mater. Struct.*, vol. 23(10), **2014**, doi: 10.1088/0964-1726/23/10/104004.

[18] P. Balakrishnan, S. Thomas, et al., "Biomaterials and biotechnological schemes utilizing TiO_2 nanotube arrays," in *Fundamental Biomaterials: Metals*, Detroit, Ed: Elsevier Ltd, pp. 193–207, **2018**.

[19] F. Zhang, J. Zhao, et al., "TiO_2-assisted photodegradation of dye pollutants II. Adsorption and degradation kinetics of eosin in TiO_2," *Appl. Catal. B Environ.*, vol. 15, pp. 147–156, **1998**, doi: 10.1016/S0926-3373(97)00043-X.

[20] W. Li, D. Li *et al.*, "Evidence for the active species involved in the photodegradation process of methyl Orange on TiO_2," *J. Phys. Chem. C*, vol. 116(5), pp. 3552–3560, **2012**, doi: 10.1021/jp209661d.

[21] F. Sauvage, F. Di Fonzo *et al.*, "Hierarchical TiO_2 photoanode for dye-sensitized solar cells," *Nano Lett.*, vol. 10(7), pp. 2562–2567, **2010**, doi: 10.1021/nl101198b.

[22] P. Roy, D. Kim, et al., "TiO_2 nanotubes and their application in dye-sensitized solar cells," *Nanoscale*, vol. 2(1), pp. 45–59, **2010**, doi: 10.1039/b9nr00131j.

[23] Y. Lai, J. Huang, *et al.*, "Recent Advances in TiO_2-Based Nanostructured Surfaces with Controllable Wettability and Adhesion," *Small*, vol. 12(16), pp. 2203–2224, **2016**, doi: 10.1002/smll.201501837.

[24] S. Banerjee, D. D. Dionysiou, et al., "Self-cleaning applications of TiO_2 by photo-induced hydrophilicity and photocatalysis," *Appl. Catal. B Environ.*, vol. 176–177, pp. 396–428, **2015**, doi: 10.1016/j.apcatb.2015.03.058.

[25] Y. H. Hu, "A highly efficient photocatalyst-hydrogenated black TiO_2 for the photocatalytic splitting of water," *Angew. Chemie - Int. Ed.*, vol. 51(50), pp. 12410–12412, **2012**, doi: 10.1002/anie.201206375.

[26] A. Galińska and J. Walendziewski, "Photocatalytic water splitting over Pt-TiO_2 in the presence of sacrificial reagents," *Energy and Fuels*, vol. 19(3), pp. 1143–1147, **2005**, doi: 10.1021/ef0400619.

[27] J. Yu, L. Qi, et al., "Hydrogen production by photocatalytic water splitting over Pt/TiO_2 nanosheets with exposed (001) facets," *J. Phys. Chem. C*, vol. 114(30), pp. 13118–13125, **2010**, doi: 10.1021/jp104488b.

[28] X. Lang, X. Chen, et al., "Heterogeneous visible light photocatalysis for selective organic transformations," *Chem. Soc. Rev.*, vol. 43(1), pp. 473–486, **2014**, doi: 10.1039/c3cs60188a.

[29] A. A. Haidry, P. Schlosser, *et al.*, "Hydrogen gas sensors based on nanocrystalline TiO_2 thin films," *Cent. Eur. J. Phys.*, vol. 9(5), pp. 1351–1356, **2011**, doi: 10.2478/s11534-011-0042-3.

[30] J. Chen, J. Zhang, et al., "Preparation and application of TiO_2 photocatalytic sensor for chemical oxygen demand determination in water research," *Water Res.*, vol. 39(7), pp. 1340–1346, **2005**, doi: 10.1016/j.watres.2004.12.045.

[31] A. Fujishima and K. Honda, "Electrochemical Photolysis of Water at a Semiconductor Electrode," *Nature*, vol. 238(5358), pp. 37–38, **1972**, doi: 10.1038/238038a0.

[32] S. Kang, S. Li, *et al.*, "Mesoporous black TiO_2 array employing sputtered Au cocatalyst exhibiting efficient charge separation and high H_2 evolution activity," *Int. J. Hydrogen Energy*, vol. 43(49), pp. 22265–22272, **2018**, doi: 10.1016/j.ijhydene.2018.10.067.

[33] M. Ni, M. K. H. Leung, et al., "A review and recent developments in photocatalytic water-splitting using TiO_2 for hydrogen production," *Renew. Sustain. Energy Rev.*, vol. 11(3), pp. 401–425, **2007,** doi: 10.1016/j.rser.2005.01.009.

[34] S. G. Ullattil, S. B. Narendranath,et al., "Black TiO_2 Nanomaterials: A Review of Recent Advances," *Chem. Eng. J.*, vol. 343, pp. 708–736, **2018**, doi: 10.1016/j.cej.2018.01.069.

[35] X. Bi, G. Du, *et al.*, "Room-temperature synthesis of yellow TiO_2 nanoparticles with enhanced photocatalytic properties," *Appl. Surf. Sci.*, vol. 511, p. 145617, **2020**, doi: 10.1016/j.apsusc.2020.145617.

[36] C. Randorn, J. T. S. Irvine, et al., "Synthesis of visible-light-activated yellow amorphous TiO_2 photocatalyst," *Int. J. Photoenergy*, vol.19, **2008**, doi: 10.1155/2008/426872.

[37] G. Liu, L. C. Yin, *et al.*, "A red anatase TiO_2 photocatalyst for solar energy conversion," *Energy*

Environ. Sci., vol. 5(11), pp. 9603–9610, **2012**, doi: 10.1039/c2ee22930g.

[38] Q. Zhu, Y. Peng, *et al.*, "Stable blue TiO_{2-x} nanoparticles for efficient visible light photocatalysts," *J. Mater. Chem. A*, vol. 2(12), pp. 4429–4437, **2014**, doi: 10.1039/c3ta14484d.

[39] J. Qiu, S. Li, *et al.*, "Hydrogenation Synthesis of Blue TiO_2 for High-Performance Lithium- Ion Batteries," *J. Phys. Chem. C, vol. 118(17), pp. 8824-8830,* **2014**, doi: dx.doi.org/10.1021/jp501819p.

[40] Y. Liu, P. Chen, *et al.*, "Grey rutile TiO_2 with long-term photocatalytic activity synthesized via two-step calcination," *Nanomaterials*, vol. 10(5), pp. 920, **2020**, doi: 10.3390/nano10050920.

[41] L. Wang, Y. Cai, et al., "A facile synthesis of brown anatase TiO_2 rich in oxygen vacancies and its visible light photocatalytic property," *Solid State Ionics*, vol. 361, pp. 115564, **2021**, doi: 10.1016/j.ssi.2021.115564.

[42] C. Fan, C. Chen, *et al.*, "Black Hydroxylated Titanium Dioxide Prepared via Ultrasonication with Enhanced Photocatalytic Activity," *Sci. Rep.*, vol. 5(1), pp. 1–10, **2015**, doi: 10.1038/srep11712.

[43] M. Zimbone, G. Cacciato *et al.*, "Hydrogenated black-TiO_x: A facile and scalable synthesis for environmental water purification," *Catal. Today*, vol. 321–322, pp. 146–157, **2019**, doi: 10.1016/j.cattod.2018.03.040.

[44] Z. Dong, D. Ding, et al., "Black Si-doped TiO_2 nanotube photoanode for high-efficiency photoelectrochemical water splitting," *RSC Adv.*, vol. 8(11), pp. 5652–5660, **2018**, doi: 10.1039/c8ra00021b.

[45] L. Andronic and A. Enesca, "Black TiO_2 Synthesis by Chemical Reduction Methods for Photocatalysis Applications," *Front. Chem.*, vol. 8, pp. 1–8, **2020**, doi: 10.3389/fchem.2020.565489.

[46] X. Chen, D. Zhao, *et al.*, "Laser-Modified Black Titanium Oxide Nanospheres and Their Photocatalytic Activities under Visible Light," *ACS Appl. Mater. Interfaces*, vol. 7(29), pp. 16070–16077, **2015**, doi: 10.1021/acsami.5b04568.

[47] X. Chen, L. Liu, et al., "Supporting Material for Increase Solar Absorption for Photocatalysis with Black Hydrogenated Titanium Dioxide Nonocrystals," *Science (80-.).*, vol. 331, pp. 746–751, **2011**, doi: 10.1126/science.1200448.

[48] H. Tan, M. Chengyu *et al.*, "A facile and versatile method for preparation of colored TiO_2 with enhanced solar-driven photocatalytic activity," *Nanoscale*, vol. 6(17), pp. 10216–10223, **2014**, doi: 10.1039/c4nr02677b.

[49] A. Naldoni, M. Allieta *et al.*, "Effect of nature and location of defects on bandgap narrowing in black TiO_2 nanoparticles," *J. Am. Chem. Soc.*, vol. 134(18), pp. 7600–7603, **2012,** doi: 10.1021/ja3012676.

[50] Z. Lu, C. T. Yip, et al., "Hydrogenated TiO_2 nanotube arrays as high-rate anodes for lithium-ion microbatteries," *Chempluschem*, vol. 77(11), pp. 991–1000, **2012**, doi: 10.1002/cplu.201200104.

[51] H. Hamad, E. Bailón-García et al., "Synthesis of TixOy nanocrystals in mild synthesis conditions for the degradation of pollutants under solar light," Appl. Catal. B Enviro., vol. 241, pp: 385-392, **2019**, doi: 10.1016/j.apcatb.2018.09.016

[52] G. Zhu, H. Yin, et al., "Black Titania for Superior Photocatalytic Hydrogen Production and Photoelectrochemical Water Splitting," ChemCatChem, vol. 7(17), pp. 2614-2619, **2015**, doi: 10.1002/cctc.201500488

[53] M. Sabzehparvar, F. Kiani, et al., "Synthesis and characterization of black amorphous titanium oxide nanoparticles by spark discharge method," *AIP Conf. Proc.*, vol. 1920(1), pp. 020046, **2018**, doi: 10.1063/1.5018978.

[54] L. R. Grabstanowicz, S. Gao, et al., "Facile oxidative conversion of TiH_2 to high-concentration Ti^{3+}-self-doped rutile TiO_2 with visible-light photoactivity," Inorg. Chem., vol. 52(7), pp. 3884–3890, **2013**, doi: 10.1021/ic3026182.

[55] Z. Wang, C. Yang, *et al.*, "H-doped black titania with very high solar absorption and excellent photocatalysis enhanced by localized surface plasmon resonance," *Adv. Funct. Mater.*, vol. 23(43),

pp. 5444–5450, **2013**, doi: 10.1002/adfm.201300486.

[56] G. Li, Z. Lian, *et al.*, "Ionothermal synthesis of black Ti^{3+}-doped single-crystal TiO_2 as an active photocatalyst for pollutant degradation and H_2 generation," *J. Mater. Chem. A*, vol. 3(7), pp. 3748–3756, **2015**, doi: 10.1039/c4ta02873b.

[57] W. Fang, M. Xing, et al., "A new approach to prepare Ti^{3+} self-doped TiO_2 via $NaBH_4$ reduction and hydrochloric acid treatment," *Appl. Catal. B Environ.*, vol. 160–161(1), pp. 240–246, **2014**, doi: 10.1016/j.apcatb.2014.05.031.

[58] N. T. K. Thanh, N. Maclean, et al., "Mechanisms of nucleation and growth of nanoparticles in solution," *Chem. Rev.*, vol. 114(15), pp. 7610–7630, **2014**, doi: 10.1021/cr400544s.

[59] H. L. Ma, J. Y. Yang, et al., "Raman study of phase transformation of TiO_2 rutile single crystal irradiated by infrared femtosecond laser," vol. 253(18), pp. 7497–7500, **2007**, doi: 10.1016/j.apsusc.2007.03.047.

[60] S. Challagulla, K. Tarafder, et al., "Structure sensitive photocatalytic reduction of nitroarenes over TiO2," *Sci. Rep.*, vol. 7(1), pp. 1–11, **2017**, doi: 10.1038/s41598-017-08599-2.

[61] D. A. H. Hanaor and C. C. Sorrell, "Review of the anatase to rutile phase transformation," *J. Mater. Sci.*, vol. 46(4), pp. 855–874, **2011**, doi: 10.1007/s10853-010-5113-0.

[62] T. Kheamrutai, P. Limsuwan, et al., "Phase Characterization of TiO_2 Powder by XRD and TEM," Nat. Sci., vol. 42(5), pp. 357-361, **2008**, doi:

[63] S. Ali Ansari, M. Mansoob Khan, et al., "Nitrogen-doped titanium dioxide (N-doped TiO_2) for visible light photocatalysis," *New J. Chem.*, vol. 40(4), pp. 3000–3009, **2016**, doi: 10.1039/x0xx00000x.

[64] M. N. Abellán, B. Bayarri, et al., "Photocatalytic degradation of sulfamethoxazole in aqueous suspension of TiO_2," *Appl. Catal. B Environ.*, vol. 74(3-4), pp. 233–241, **2007**, doi: 10.1016/j.apcatb.2007.02.017.

[65] O. Porcar-Santos, A. Cruz-Alcalde, et al., "Photocatalytic degradation of sulfamethoxazole using TiO_2 in simulated seawater: Evidence for direct formation of reactive halogen species and halogenated by-products," *Sci. Total Environ.*, vol. 736, pp. 139605, **2020**, doi: 10.1016/j.scitotenv.2020.139605.

11. ACRONYMS

nm: Nanometer

NPs: Nanoparticles

UV: Ultraviolet

NIR: Near Infrared

NMs: Nanomaterials

VB: Valence band

CB: Conduction band

h^+: Positive holes

e^-: Photogenerated electrons

TTIP: Titanium (IV) isopropoxide

SMX: Sulfamethoxazole

SEM: Scanning electron microscope

EDS: Energy dispersive X-ray spectroscopy

FESEM: Field Emission Electron Microscope

CCD: Charge-coupled device

XRD: X-ray diffraction

kV: kilovolt

mA: milliamperes

HPLC: High-performance liquid chromatography

µm: micrometres

MAUD: Material analysis using diffraction

PL: Photoluminescence

APPENDICES

APPENDIX 1: FESEM PICTURES

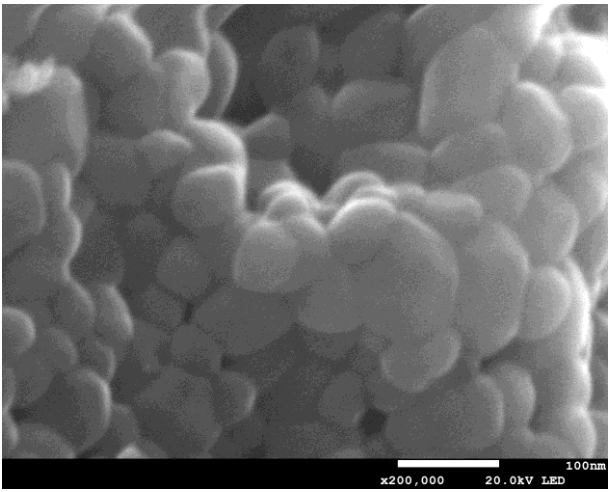

Figure 19: FESEM picture at 200.000 magnifications of TiO_2 NPs synthetized by sol-gel method, with NaOH addition and dyalisis neutralization after all heat treatments.

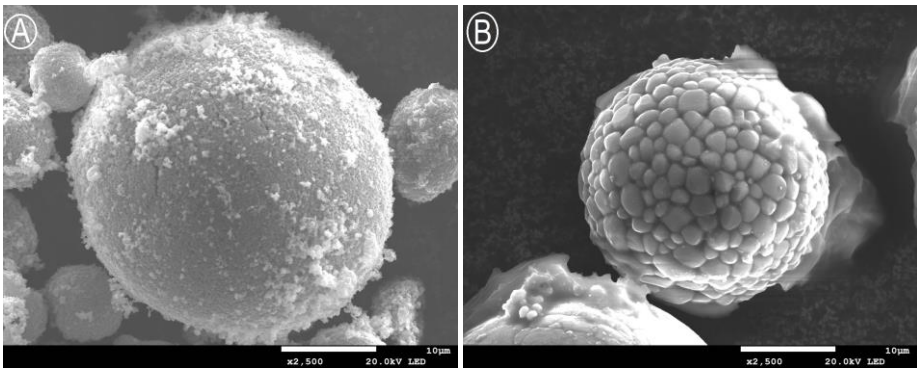

Figure 20: FESEM picture at 2.500 magnifications of TiO_2 after the heat treatment under a reductant atmosphere with $NaBH_4$: A) Anatase and B) Rutile

APPENDIX 2: DIALYSIS PROCESS

Figure 20: Dialysis process A) After neutralizing for one week (gel), B) After heating for one day at 100 ºC (appearently red TiO_2) , and C) After grinding it in a mortar (yellow TiO_2)